molecular systems, makes doubly and highly multiply charged anions a promising area of research. The connection of gas-phase multiply charged anions to those known to exist in the condensed state likewise offers an exciting challenge for future research.

New developments in high-resolution laser photodetachment spectroscopy should allow accurate measurement of atomic and molecular EAs. Likewise, the explosive technical progress as well as the price reduction in the field of supercomputing hardware devices now routinely makes amenable accurate large-scale computations of the EA for rather large molecular systems by elaborate theoretical techniques. In many critical cases, the recent progress already has allowed experiment and theory to converge to commonly accepted (final) results.

REFERENCES

1. H. S. W. Massey, *Negative Ions* (Cambridge Univ. Press, London, ed. 3, 1976).
2. ———, *Adv. At. Mol. Opt. Phys.* **15**, 1 (1979).
3. H. Hotop and W. C. Lineberger, *J. Phys. Chem. Ref. Data* **14**, 731 (1985).
4. D. R. Bates, *Adv. At. Mol. Opt. Phys.* **27**, 1 (1990).
5. R. N. Compton, *Negative Ions (Atomic Negative Ions)*, V. Esaulov, Ed. (Cambridge Univ. Press, Cambridge, in press).
6. I. H. Bauman, E. Heinicke, H. J. Kaiser, K. Bethge, *Nucl. Instrum. Methods* **95**, 389 (1971).
7. L. Frees, E. Heinicke, W. S. Koski, *ibid.* **159**, 105 (1979).
8. L. M. Branscomb and W. L. Fite, *Phys. Rev.* **93**, 651 (1954).
9. K. R. Lykke, K. K. Murray, W. C. Lineberger, *Phys. Rev. A* **43**, 6104 (1991).
10. C. L. Pekeris, *Phys. Rev.* **112**, 1649 (1958); *ibid.* **126**, 1470 (1962).
11. H. Haberland, T. Kolar, T. Reiners, *Phys. Rev. Lett.* **63**, 1219 (1989).
12. R. N. Compton, P. W. Reinhardt, C. D. Cooper, *J. Chem. Phys.* **63**, 3821 (1975).
13. J. D. Watts and R. J. Bartlett, *ibid.* **97**, 3445 (1992).
14. N. Bartlett, *Angew. Chem. Int. Ed. Engl.* **7**, 433 (1968); R. N. Compton, P. W. Reinhardt, C. D. Cooper, *J. Chem. Phys.* **68**, 2023 (1978).
15. R. N. Compton, *J. Chem. Phys.* **66**, 4478 (1977).
16. G. L. Gutsev and A. I. Boldyrev, *Chem. Phys.* **56**, 277 (1981); *Chem. Phys. Lett.* **108**, 250 (1984).
17. C. Yannovleas and U. Landman, *Phys. Rev. B* **48**, 8376 (1993).
18. L. S. Wang, J. Conceicao, C. Jin, R. E. Smalley, *Chem. Phys. Lett.* **182**, 5 (1991).
19. C. Jin *et al.*, *Phys. Rev. Lett.* **73**, 2821 (1994).
20. J. D. Jackson, *Classical Electrodynamics* (Wiley, New York, 1962), p. 31.
21. N. Bohr, *The London, Edinburgh and Dublin Philosophical Magazine and Journal of Science* (sixth series, July 1913).
22. E. H. Lieb, *Phys. Rev. Lett.* **52**, 315 (1984); *Phys. Rev.* **29**, 3018 (1984).
23. F. Robicheaux, R. P. Wood, C. H. Greene, *Phys. Rev. A.* **49**, 1866 (1994).
24. W. K. Stuckey and R. W. Kiser, *Nature* **211**, 963 (1966).
25. R. W. Kiser, *Top. Curr. Chem.* **83**, 89 (1979).
26. R. N. Compton, *Negative Ions (Multiply Charged Negative Ions)*, V. Esaulov, Ed. (Cambridge Univ. Press, Cambridge, in press); in *Photophysics and Photochemistry in the Vacuum Ultraviolet*, S. P. McGlynn *et al.*, Eds. (Reidel, Dordrecht, Netherlands, 1985), p. 261.
27. R. C. Dougherty, *J. Chem. Phys.* **50**, 1896 (1969).
28. W. P. M. Maas and N. M. M. Nibbering, *Int. J. Mass Spectrom. Ion Processes* **88**, 257 (1989).
29. H. W. Kroto, J. R. Heath, S. C. O'Brien, R. F. Curl, R. E. Smalley, *Nature* **318**, 162 (1985).
30. R. L. Hettich, R. N. Compton, R. H. Ritchie, *Phys. Rev. Lett.* **67**, 1242 (1991).
31. P. A. Limbach *et al.*, *J. Chem. Soc.* **113**, 6795 (1991).
32. A. Mandelbaum and A. Etinger, *Org. Mass Spectrom.* **28**, 487 (1993).
33. A. H. H. Chang, W. C. Ermler, R. M. Pitzer, *J. Phys. Chem.* **95**, 9288 (1991).
34. C. Yannouleas and U. Landman, *Chem. Phys. Lett.* **217**, 175 (1994).
35. R. L. Martin and J. P. Ritchie, *Phys. Rev. B* **48**, 4845 (1993).
36. M. R. Pederson and A. A. Quong, *ibid.* **46**, 13584 (1992).
37. K. Leiter, W. Ritter, A. Stamatovic, T. D. Märk, *Int. J. Mass Spectrom. Ion Processes* **68**, 341 (1986).
38. S. N. Schauer, P. Williams, R. N. Compton, *Phys. Rev. Lett.* **65**, 625 (1990).
39. T. Sommerfeld, M. K. Scheller, L. S. Cederbaum, *Chem. Phys. Lett.* **209**, 216 (1993); *J. Phys. Chem.* **98**, 8914 (1994).
40. D. W. Arnold, S. E. Bradforth, T. N. Kitsopoulos, D. M. Neumark, *J. Chem. Phys.* **95**, 8753 (1991).
41. P. Pyykkö and N. Runeberg, *J. Mol. Struct. Theochem* **234**, 279 (1991); *Chem. Commun.* **1991**, 547 (1991); P. Pyykkö and Y. Zhao, *Chem. Phys. Lett.* **177**, 103 (1991).
42. A. I. Boldyrev and J. Simons, *J. Chem. Phys.* **98**, 4745 (1993).
43. R. Janoschek, *Z. Anorg. Allg. Chem.* **616**, 101 (1992); A. T. Blades and P. Kebarle, *J. Am. Chem. Soc.* **116**, 10761 (1994).
44. M. K. Scheller *et al.*, in preparation.
45. H.-G. Weikert and L. S. Cederbaum, *J. Chem. Phys.* **99**, 8877 (1993).
46. M. K. Scheller and L. S. Cederbaum, *J. Phys. B* **25**, 2257 (1992); *J. Chem. Phys.* **99**, 441 (1993).
47. E. Miyoshi *et al.*, *J. Phys. Chem.* **89**, 4193 (1988); E. Miyoshi and Y. Sakai, *J. Chem. Phys.* **89**, 7363 (1988).
48. M. V. Korobov *et al.*, *Int. J. Mass Spectrom. Ion Processes* **87**, 13 (1989).
49. G. L. Gutsev, *Chem. Phys. Lett.* **184**, 305 (1991).
50. C. S. Ewig and J. R. van Wazer, *J. Am. Chem. Soc.* **112**, 109 (1990).
51. H.-G. Weikert, L. S. Cederbaum, F. Tarantelli, A. I. Boldyrev, *Z. Phys. D.* **18**, 299 (1991).
52. M. K. Scheller and L. S. Cederbaum, *Chem. Phys. Lett.* **216**, 141 (1993).
53. C. M. Whitehouse, R. N. Dreyer, M. Yamashita, J. B. Fenn, *Anal. Chem.* **57**, 675 (1985); M. Yamashita and J. B. Fenn, *J. Phys. Chem.* **88**, 4451 (1984).
54. T. R. Covey, A. P. Bruins, J. D. Henion, *Org. Mass Spectrom.* **23**, 178 (1988).
55. L. O. G. Weidolf, E. D. Lee, J. D. Henion, *Biomed. Environ. Mass Spectrom.* **15**, 283 (1988).
56. S. T. F. Lai and C. A. Evans Jr., *Org. Mass Spectrom.* **13**, 733 (1978).
57. G. L. Gutsev and A. I. Boldyrev, *J. Phys. Chem.* **94**, 2256 (1990).
58. M. K. Scheller and L. S. Cederbaum; *J. Chem. Phys.* **100**, 8934 (1994); *ibid.*, p. 8943; *ibid.* **101**, 3962 (1994).

RESEARCH ARTICLES

Reconstitution of I_{KATP}: An Inward Rectifier Subunit Plus the Sulfonylurea Receptor

Nobuya Inagaki,* Tohru Gonoi,* John P. Clement IV, Noriyuki Namba, Johji Inazawa, Gabriela Gonzalez, Lydia Aguilar-Bryan, Susumu Seino,† Joseph Bryan

A member of the inwardly rectifying potassium channel family was cloned here. The channel, called BIR (Kir6.2), was expressed in large amounts in rat pancreatic islets and glucose-responsive insulin-secreting cell lines. Coexpression with the sulfonylurea receptor SUR reconstituted an inwardly rectifying potassium conductance of 76 picosiemens that was sensitive to adenosine triphosphate (ATP) (I_{KATP}) and was inhibited by sulfonylureas and activated by diazoxide. The data indicate that these pancreatic β cell potassium channels are a complex composed of at least two subunits—BIR, a member of the inward rectifier potassium channel family, and SUR, a member of the ATP-binding cassette superfamily. Gene mapping data show that these two potassium channel subunit genes are clustered on human chromosome 11 at position 11p15.1.

ATP-sensitive potassium currents, I_{KATP}, were discovered in cardiac muscle (*1*) and later found in pancreatic β cells, pituitary tissue, skeletal muscle, brain, and vascular and nonvascular smooth muscle (*2*). I_{KATP} functions in secretion and muscle contraction by coupling metabolic activity to membrane potential. In pancreatic β cells, ATP-sensitive potassium channels (K_{ATP} channels) are crucial for the regulation of glucose-induced insulin secretion (*2*, *3*) and are the target for the sulfonylureas, oral hypoglycemic agents widely used in the treatment of noninsulin-dependent diabetes mellitus (NIDDM) (*4*), and for diazoxide, a potassium channel opener. The sulfonylurea receptor (SUR) is a member of the ATP-binding cassette superfamily (*5*) with multiple transmembrane-spanning domains and two potential nucleotide-binding folds. Truncations of SUR that remove the second nucleotide-binding fold cause familial persistent hyperinsulinemic hypoglycemia of infancy (PHHI), a rare disorder of

glucose homeostasis characterized by unregulated insulin secretion despite severe hypoglycemia (6). Although these observations imply that SUR is closely associated with, or even a subunit of, K_{ATP} channels, expression of SUR alone has not produced a measurable I_{KATP} (5).

Cloning of a member of the inward rectifier family, BIR. A member of the small inward rectifier family, uK_{ATP}-1 (Kir6.1), has been cloned and is expressed in various tissues including pancreatic islets, but not insulin-secreting cell lines (*7*). Because a similar subunit might be expressed in β cells and insulin-secreting cell lines and because several genes encoding inward rectifiers lack introns (*8*), a human genomic library was screened for novel clones (*9*). Seventeen positive λ clones were sequenced, and five of them share the sequence of the human uK_{ATP}-1 gene; four clones encoded a distinct protein similar to uK_{ATP}-1, designated BIR (for β cell inward rectifier family member). This subunit is Kir6.2 in the nomenclature of Chandy and Gutman (*10*). The sequence of the longest clone revealed a single open reading frame encoding a 390–amino acid protein with two putative transmembrane segments (Fig. 1). Cloning and sequencing of a mouse homolog of BIR (mBIR) isolated from an insulin-secreting cell line complementary DNA (cDNA) library (*9*) revealed a single open reading frame encoding a 390–amino acid protein (Fig. 1) with 96 percent amino acid identity with human BIR (hBIR), which confirms that the gene encoding human BIR is intronless in the protein-coding region. The predicted amino acid sequences of hBIR versus mBIR show 71 percent identity (82 percent similarity) with rat uK_{ATP}-1 and 41, 46, 42, and 44 percent identity with ROMK1 (*11*), IRK1 (*12*), GIRK1 (*13*), and cK_{ATP}-1/CIR, respectively (*14*).

This suggests that BIR is in the same subfamily as uK_{ATP}-1, an observation that other structural features of BIR confirm: The highly conserved H5 region motif, Gly-Tyr-Gly, found in all inwardly rectifying potassium channels identified to date (*15*) is Gly-Phe-Gly in both BIR and uK_{ATP}-1. The inward rectifiers, IRK1 and GIRK1, have an aspartic acid (Asp) in the second transmembrane segment (residue 172 of IRK1) that determines their strong rectification character (*8*, *16*), whereas the weak rectifiers ROMK1, cK_{ATP}-1, and uK_{ATP}-1 have an asparagine (Asn) residue at the corresponding position. An Asn residue at this position in BIR (residue 153) suggests it should form a weak rectifier.

```
        #                                 #
hBIR  MLSRKGIIPEEYVLTRLAEDPAEPRYRARQRRARFVSKKGNCNVAHKNIREQGRFLQDVFTTLVDLKWPH   70
mBIR                             T E                                          70

         <---------M1---------->                       <-------H5------->
hBIR  TLLIFTMSFLCSWLLFAMAWWLIAFAHGDLAPSEGTAEPCVTSIHSFSSAFLFSIEVQVTIGFGGRMVTE  140
mBIR                        V             G   NV                            140

          <---------M2---------->
hBIR  ECPLAILSLIVQNIVGLMINAIMLGCIFMKTAQAHRRAETLIFSKHAVIALRHGRLCFMLRVGDLRKSMI  210
mBIR         I                                         T                    210
                                                       #

                   *
hBIR  ISATIHMQVVRKTTSPEGEVVPLHQVDIPMENGVGGNSIFLVAPLIIYHVIDANSPLYDLAPSDLHHHQD  280
mBIR                                         G              S               280

                                                             #        #
hBIR  LEIIVILEGVVETTGITTQARTSYLADEILWGQRFVPIVAEEDGRYSVDYSKFGNTIKVPTPLCTARQLD  350
mBIR                                                                        350

                  #        *
hBIR  EDHSLLEALTLASARGPLRKRSVPMAKAKPKFSISPDSLS      390
mBIR    R   D      S         AV                   390
```

Fig. 1. Comparison of the amino acid sequences of human and mouse BIR. Amino acids are indicated in the single-letter code. The amino acid residues of mouse BIR (mBIR) different from those of human BIR (hBIR) sequences are shown below that of hBIR. Predicted transmembrane (M1 and M2) and pore (H5) segments are indicated (*31*). Potential cyclic AMP–dependent protein kinase phosphorylation sites and protein kinase C–dependent phosphorylation sites are indicated by * and #, respectively. Abbreviations for the amino acid residues are as follows: A, Ala; C, Cys; D, Asp; E, Glu; F, Phe; G, Gly; H, His; I, Ile; K, Lys; L, Leu; M, Met; N, Asn; P, Pro; Q, Gln; R, Arg; S, Ser; T, Thr; V, Val; W, Trp; and Y, Tyr.

Northern (RNA) analysis (Fig. 2) revealed that BIR messenger RNA (mRNA) is expressed in large amounts in pancreatic islets, the glucose-responsive insulin-secreting cell lines MIN6 (mouse) and HIT-T15 (hamster), and the glucagon-secreting α cell line αTC-6 (mouse); it is expressed in smaller amounts in heart, skeletal muscle, brain, and the insulin-secreting cell line RINm5F (rat) (*17*). These tissues and cell lines have I_{KATP} (*2*, *18*, *19*). BIR mRNA was not expressed in the other tissues and cell lines examined (Fig. 2). When the same nylon membranes were again probed with ^{32}P-labeled SUR cDNA from hamsters (*5*), SUR mRNA was coexpressed in the same tissues and pancreatic islet–derived cell lines as BIR mRNA (Fig. 2). SUR mRNA is expressed in small amounts in brain but is absent or expressed only in very small amounts in heart and skeletal muscle.

With the use of fluorescence in situ hybridization (FISH), we observed that the human BIR gene maps to the short arm of human chromosome 11 (*20*). Giemsa staining of 30 (pro)metaphase figures of chromosome 11 produced "G-banding" patterns that localized the twin-spot signals from the fluorescent human BIR probe to 11p15.1. The sequence obtained from one λ clone at the 3′ end of the gene encoding SUR matches a part of the gene encoding BIR; a long polymerase chain reaction (PCR) with a sense primer (*21*) near the 3′ end of the SUR gene and an antisense primer (*21*) near the 5′ end of the BIR gene amplified an approximately 4.5-kilobase fragment. Thus, the two genes are clustered at 11p15.1, with the BIR gene immediately 3′ of the SUR gene.

Reconstitution of I_{KATP} from BIR and SUR. Coexpression of mouse BIR (mBIR)

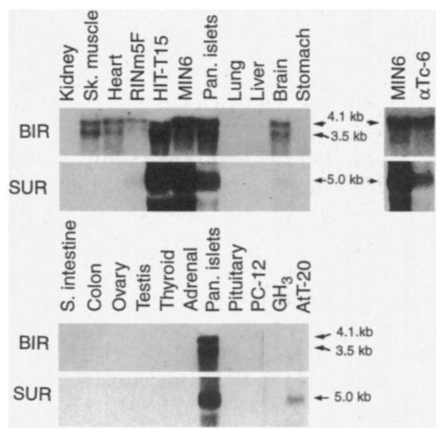

Fig. 2. Northern analysis of BIR and SUR mRNA in various rat tissues and hormone-secreting cell lines. The sizes of the hybridized transcripts are indicated. The sizes of the transcripts of BIR are 4.1 and 3.5 kb, 4.1 kb, and 4.0 and 3.5 kb in rat, mouse, and hamster, respectively. The size of the transcript of SUR is 5.0 kb. For autoradiography, the nylon membranes were exposed to x-ray film with an intensifying screen at −80°C for 2 days. BIR mRNA could be detected in small amounts in the pituitary and the pituitary-derived AtT-20 cell line with a longer exposure (12 and 4 days, respectively); SUR mRNA could also be detected in small amounts in the pituitary with a 4-day exposure. The αTc-6 RNA was analyzed separately; MIN6 RNA was included for comparison. Sk., skeletal; Pan., pancreatic; and S., small.

N. Inagaki, N. Namba, and S. Seino are in the Division of Molecular Medicine, Center for Biomedical Science, Chiba University School of Medicine, Chuo-ku, Chiba 260, Japan. T. Gonoi is in the Research Center for Pathogenic Fungi and Microbial Toxicoses, Chiba University, Chuo-ku, Chiba 260, Japan. J. P. Clement IV, G. Gonzalez, L. Aguilar-Bryan, and J. Bryan are in the Departments of Cell Biology and Medicine, Baylor College of Medicine, Houston, TX 77030, USA. J. Inazawa is in the Department of Hygiene, Kyoto Prefectural University of Medicine, Kamigyo-ku, Kyoto 602, Japan.

*These authors contributed equally to this study.
†To whom correspondence should be addressed.

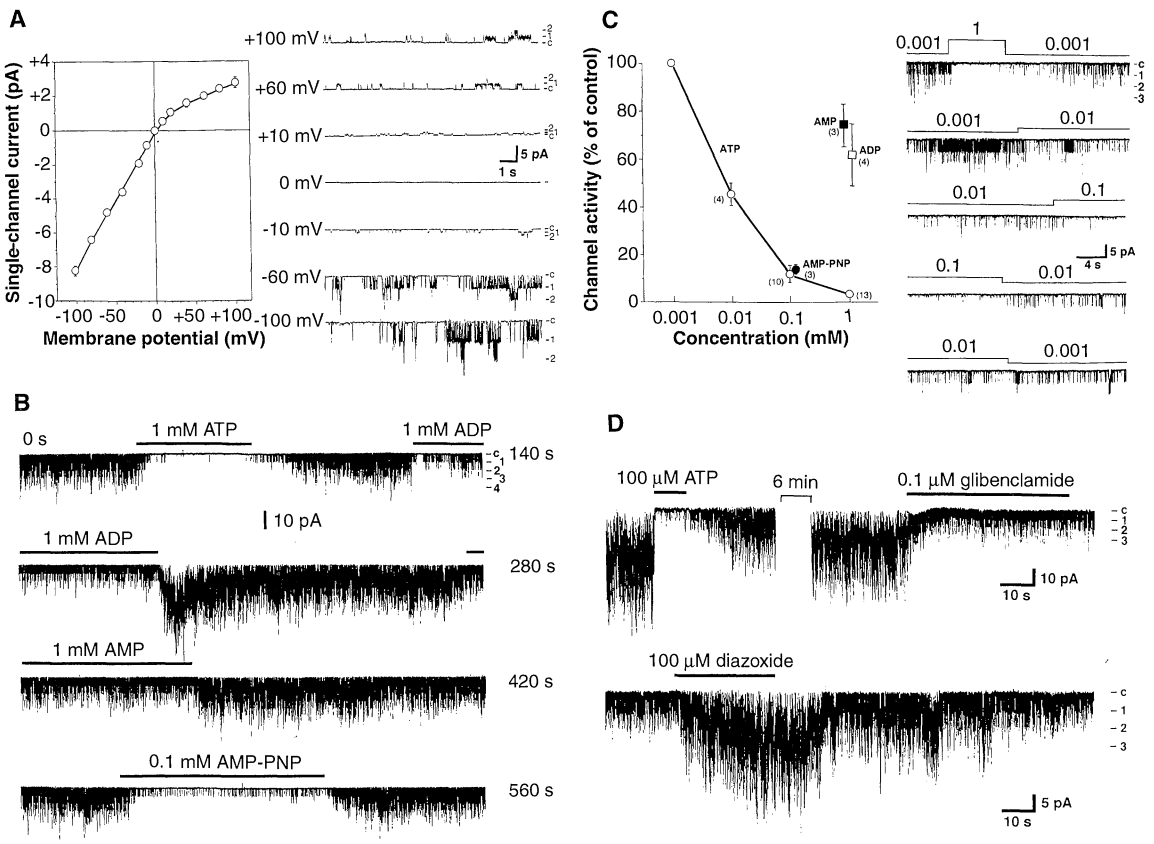

Fig. 3. Electrophysiological recording from COS-1 cells coexpressing mBIR and haSUR. (**A**) Left, inwardly rectifying property of BIR channel ($n = 6$). Right, representative traces from single-channel recordings in the inside-out mode at various holding potentials. (**B**) Effects of ATP and its analogs on channel activity. Representative traces of the excised inside-out patches are shown. Channel activity was inhibited by 1 mM dipotassium ATP and by 0.1 mM AMP-PNP, a nonhydrolyzable ATP analog. ADP (1 mM) and AMP (1 mM) in the presence of 1 μM dipotassium ATP slightly suppressed channel activity. (**C**) Left, dose-dependent effect of ATP and its analogs on channel activity. Channel activity was calculated by integrating current flow during the channel openings and dividing the integral by the total sampling time (generally 20 to 40 s). The channel activity at each concentration of the agents is expressed as a percent of the control (at 1 μM dipotassium ATP). Right, representative traces at the indicated ATP concentrations (mM). The numbers in parentheses give the number of patches analyzed for each concentration. [See (*22, 23*) for details of the transfection.] (**D**) Effects of glibenclamide (0.1 μM) and diazoxide (100 μM) on channel activity. Representative traces are shown. In (B) through (D), horizontal bars indicate application periods of the agents. Membrane potential was held at −60 mV, unless otherwise noted. Values are means ± SEM. The numbers to the right of the traces indicate the numbers of open channels.

and hamster SUR (haSUR) in COS-1 and COSm6 cells generated potassium currents that we characterized by single-channel patch-clamp (*22*) and $^{86}Rb^+$ efflux methods (*23*). The characteristics of the single-channel conductances of mBIR and haSUR cotransfectants were analyzed (Fig. 3). In the presence of 140 mM potassium (K^+) on both sides of the membrane, the current-voltage relation revealed a weak inward rectification in the presence of 2 mM magnesium (Mg^{2+}) in the intracellular solution with a reversal potential of +0.1 mV ($n = 6$) (Fig. 3A), a value close to the theoretical K^+ equilibrium potential. The single-channel conductance was calculated to be 76.4 ± 1.0 pS at a membrane potential of −60 mV ($n = 19$, mean ± SE). The K^+ conductance was completely inhibited by 1 mM ATP (Fig. 3B) and suppressed by 0.1 mM adenyl-5′-yl imidodiphosphate (AMP-PNP). Channel activity was slightly inhibited by 1 mM adenosine diphosphate (ADP), or 1 mM adenosine monophosphate (AMP), in the presence of 1 μM ATP (Fig. 3, B and C).

The ATP inhibition of channel activity was dependent on the dose, with a half-maximal value of 10 μM (Fig. 3C). ATP-sensitive channels were observed in 25 out of 147 random patches (17.0 percent) in cotransfected COS-1 cells. In contrast, in untransfected COS-1 cells (4 out of 188 patches, or 2.1 percent), COS-1 cells transfected with mBIR alone (5 out of 200 patches, or 2.5 percent), or COS-1 cells transfected with haSUR alone (1 out of 75 patches, or 1.3 percent), only ATP-insensitive potassium currents of various conductances between 30 and 300 pS were found. Glibenclamide (*24*) (0.1 μM) blocked the reconstituted K_{ATP} channels (Fig. 3D), and diazoxide (100 μM), a potent opener of β cell K_{ATP} channels (*25*), stimulated activity (Fig. 3D).

$^{86}Rb^+$ efflux measurements confirmed the results obtained with single channels at a macroscopic level and directly linked the reconstituted potassium currents to the intracellular concentration of ATP. Transfection of COSm6 cells with either plasmid alone had no effect on basal efflux and produced no additional currents upon addition of metabolic inhibitors (Fig. 4A). An endogenous COSm6 cell current was inhibited by metabolic poisoning (Fig. 4A). Cotransfection with mBIR and haSUR increased basal $^{86}Rb^+$ efflux above that seen in controls transfected with β-galactosidase (Fig. 4, A and B). Metabolic poisoning with oligomycin (2.5 μg/ml) and 2 mM 2-deoxyglucose stimulated efflux beyond basal levels (Fig. 4B) despite the simultaneous inhibition of the endogenous COSm6 cell current (Fig. 4A). Efflux through the reconstituted channels was inhibited by glibenclamide (Fig. 4B) and was activated by diazoxide in the absence of metabolic inhibitors (Fig. 4C). The dose responses (Fig. 4D) for activation by diazoxide (half-maximal at 60 μM) and inhibition by glibenclamide (half-maximal at 1.8 nM) and tolbutamide (half-maximal at 32 μM) were those expected for β cell I_{KATP} (*2*).

Distinct potassium channel activity was observed in *Xenopus laevis* oocytes co-injected with mBIR and haSUR complementary RNAs (cRNAs) (*26*). With 90 mM K^+ in the external solution, inward membrane currents were increased by 100 μM diazoxide and decreased by 0.1 μM glibenclamide (16 out of 23 oocytes) (Fig. 5). The inhibitory effect of glibenclamide was not reversible when the drug was washed away or by addition of another dose of diazoxide. Oocytes injected with H_2O ($n = 32$), mBIR cRNA alone ($n = 15$), or haSUR cRNA

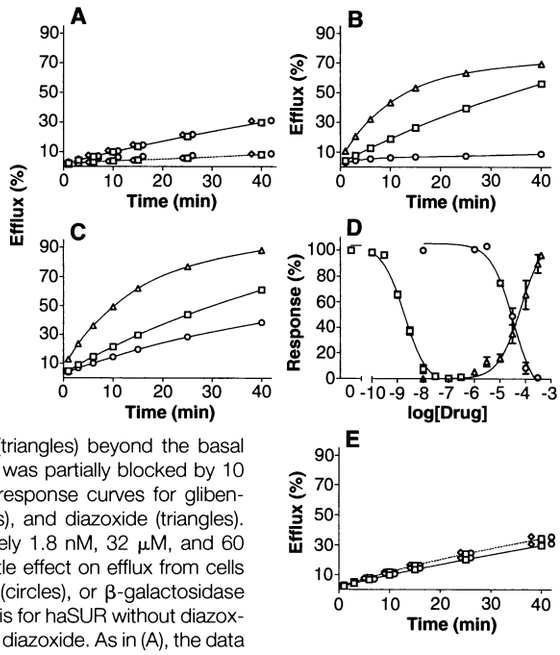

Fig. 4. $^{86}Rb^+$ efflux from COSm6 cells coexpressing mBIR and haSUR. (**A**) Basal efflux from cells expressing only mBIR (diamonds), haSUR (circles), or β-galactosidase (squares) in the absence (top line) or presence (bottom line) of metabolic inhibitors. The data points are tightly clustered; therefore, the symbols have been offset +/− 1 or 2 min for clarity (**B**) Efflux from cells coexpressing mBIR and haSUR. Basal efflux (squares) was greater than that shown in (A) and was increased in the presence of metabolic inhibitors (triangles). The efflux activated by metabolic inhibitors was blocked by 1 μM glibenclamide (circles). (**C**) Diazoxide (200 μM) increased efflux (triangles) beyond the basal level (squares). This increased current was partially blocked by 10 μM glibenclamide (circles). (**D**) Dose-response curves for glibenclamide (squares), tolbutamide (circles), and diazoxide (triangles). Half-maximal values were approximately 1.8 nM, 32 μM, and 60 μM, respectively. (**E**) Diazoxide had little effect on efflux from cells expressing mBIR (diamonds), haSUR (circles), or β-galactosidase alone (squares). The solid (bottom) line is for haSUR without diazoxide; the dotted (top) line is with 200 μM diazoxide. As in (A), the data points are tightly clustered and the symbols have been offset +/− 1 or 2 min for clarity. The error bars are standard deviations. [See (*22, 23*) for details of the transfection.]

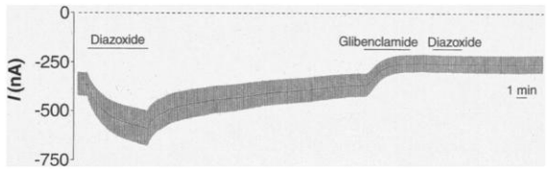

Fig. 5. A representative trace of whole-cell recording from *Xenopus laevis* oocytes co-injected with in vitro–synthesized mBIR cRNA and haSUR cRNA. The effect of 100 μM diazoxide and 0.1 μM glibenclamide on membrane currents is shown. On achieving a stable state after clamping at −60 mV (not shown in the figure), alternate voltage pulses of ±10 mV and 100-ms duration were applied every 5 s. A scale for the current amplitude is indicated. The dotted horizontal line indicates the zero current level. Horizontal bars indicate the application periods of the agents.

alone (n = 16) did not respond to diazoxide or glibenclamide (*27*). Similar effects of diazoxide and glibenclamide on potassium currents were further confirmed by whole-cell recordings of COS-1 cells coexpressing mBIR and haSUR (*28*).

These findings demonstrate that BIR and SUR reconstitute the main characteristic features of the ATP-sensitive potassium current I_{KATP} described in pancreatic β cells (*29*) and indicate that native β cell K_{ATP} channels are a complex composed of at least two subunits, BIR and SUR, with unknown stoichiometry. Because neither protein alone can function as a channel, we propose to name the subunits K_{ATP}-α for BIR and K_{ATP}-β for SUR to reflect their function as subunits of I_{KATP}. We assume that K_{ATP}-β, which binds sulfonylureas with high affinity and has two potential nucleotide-binding folds, activates K_{ATP}-α, the silent inward rectifier, and confers ATP and sulfonylurea sensitivity on I_{KATP}. Whether one or both polypeptides form the potassium selective pore is unknown, as is the binding site for the potassium channel opener diazoxide. These results imply that mutations in K_{ATP}-α, like those in K_{ATP}-β, will give rise to PHHI. The reconstitution of I_{KATP} provides a means for the molecular characterization of this channel and for understanding its role in disorders of glucose homeostasis, including diabetes mellitus and PHHI.

REFERENCES AND NOTES

1. A. Noma, *Nature* **305**, 147 (1983).
2. F. M. Ashcroft, *Annu. Rev. Neurosci.* **11**, 97 (1988).
3. D. L. Cook, L. S. Satin, M. L. J. Ashford, C. N. Hales, *Diabetes* **37**, 495 (1988).
4. S. J. H. Ashcroft and F. M. Ashcroft, *Biochim. Biophys. Acta* **1175**, 45 (1992).
5. L. Aguilar-Bryan *et al., Science* **268**, 423 (1995).
6. P. M. Thomas *et al., ibid.*, p. 426.
7. N. Inagaki *et al., J. Biol. Chem.* **270**, 5691 (1995).
8. P. R. Stanfield *et al., J. Physiol. (London)* **478**, 1 (1994); N. Inagaki *et al.*, unpublished data.
9. Seven hundred thousand plaques of a λFIXII human genomic library (Stratagene) were screened with the use of a ^{32}P-labeled rat uK_{ATP}-1 full-length cDNA (*7*) probe under standard hybridization conditions (*30*). The membranes were washed with 2× SSC (where SSC is 150 mM NaCl and 15 mM sodium citrate, pH 7.0) plus 0.1 percent SDS at 42°C for 30 min. A ^{32}P-labeled DNA fragment encoding human BIR (hBIR) (nucleotides +166 to +1421 relative to the translation start site of the gene encoding hBIR) was used as a probe to screen 7 × 10^5 plaques of a mouse insulin-secreting cell line (MIN6) cDNA library [N. Inagaki *et al., Proc. Natl. Acad. Sci. U.S.A.* **91**, 2679 (1994)] under standard hybridization conditions, followed by washing with 0.1× SSC plus 0.1 percent SDS at 50°C for 1 hour. Both strands of DNA were sequenced by dideoxynucleotide chain termination after appropriate DNA fragments were subcloned into M13mp18, M13mp19 (Toyobo, Osaka, Japan), or pGEM3Z (Promega, Madison, WI).
10. K. G. Chandy and G. A. Gutman, *Trends Pharmacol. Sci.* **14**, 434 (1993).
11. K. Ho *et al., Nature* **362**, 31 (1993).
12. Y. Kubo, T. J. Baldwin, Y. N. Jan, L. Y. Jan, *ibid.*, p. 127.
13. Y. Kubo, E. Reuveny, P. A. Slesinger, Y. N. Jan, L. Y. Jan, *ibid.* **364**, 802 (1993); N. Dascal *et al., Proc. Natl. Acad. Sci. U.S.A.* **90**, 10235 (1993).
14. M. L. J. Ashford, C. T. Bond, T. A. Blair, J. P. Adelman, *Nature* **370**, 456 (1994); G. Krapivinsky *et al., ibid.* **374**, 135 (1995).
15. M. J. Sutcliffe and P. R. Stanfield, *ibid.* **369**, 616 (1994); L. Y. Jan and Y. N. Jan, *ibid.* **371**, 119 (1994); I. D. Kerr and M. S. P. Sansom, *ibid.* **373**, 112 (1995).
16. Z. Lu and R. MacKinnon, *ibid.* **371**, 243 (1994); B. A. Wible, M. Taglialatela, E. Ficker, A. M. Brown, *ibid.*, p. 246.
17. Total RNA (20 μg) from the various tissues and cell lines except for the pituitary and thyroid (10 μg each) was denatured with formaldehyde, subject to electrophoresis on a 1 percent agarose gel, and transferred to a nylon membrane. Hybridization was carried out under standard hybridization conditions with the ^{32}P-labeled hBIR DNA fragment (*9*) and a haSUR DNA fragment (nucleotides −33 to +2325 relative to the translation start site of the haSUR cDNA) as probes. Membranes were washed with 0.1× SSC plus 0.1 percent SDS at 50°C for 1 hour.
18. A. S. Rajan *et al., J. Biol. Chem.* **268**, 15221 (1993).
19. T. Gonoi *et al.*, unpublished data.
20. Fluorescence in situ hybridization was performed essentially as described [J. Inazawa, H. Saito, T. Ariyama, T. Abe, Y. Nakamura, *Genomics* **17**, 153 (1993)]. Briefly, human (pro)metaphase chromosomes were prepared from normal male lymphocytes; the thymidine synchronization, bromodeoxyuridine release technique was used to delineate G bands. Before hybridization, chromosomes were stained in Hoechst 33258 and irradiated with ultraviolet light. Recombinant λ DNA containing the gene encoding hBIR was labeled with biotin-16-deoxyuridine triphosphate by nick-translation and hybridized to denatured chromosomes at a concentration of 25 ng/μl in 50 percent formamide, 10 percent dextran sulfate (Sigma), and *Escherichi coli* transfer RNA (2 μg/μl). Hybridization signals were detected with fluorescein isothiocyanate (FITC)–avidin (Boehringer Mannheim GmbH, Mannheim, Germany), and chromosomes were counterstained with propidium iodide (1 μg/ml). The precise signal position was determined by the delineation of G-banding patterns.
21. The primers used to amplify the intervening genomic region between the genes encoding hSUR and hBIR were (sense primer in the 3′ end of the SUR gene) 5′-CATCGAGTGCACACCAT-3′ and (antisense primer in the 5′ end of the BIR gene) 5′-GTGTCAGCACGTATTCCTCG-3′. Amplification was done with ELONGASE reagents (Life Technologies, Gaithersburg, MD) for 30 cycles of 55°C for 30 s, 72°C for 10 min, and 94°C for 30 s.
22. COS-1 cells were plated at a density of 3 × 10^5 per dish (35 mm in diameter) and cultured in Dulbecco's modified Eagle's medium (DMEM) supplemented with fetal calf serum (10 percent). A full-length mBIR cDNA and a full-length haSUR cDNA were subcloned into the mammalian expression vectors pCMV6b and pCMV6c (*30*), respectively (designated pCMVmBIR and pCMVhaSUR, respectively). pCMVmBIR alone (1 μg), pCMVhaSUR alone (1 μg), or pCMVmBIR (1 μg) and pCMVhaSUR (1 μg) were transfected into COS-1 cells with lipofectamine and Opti-MEM I reagents (Life Technologies) and pAdVantage (Promega) according to the manufacturer's instructions. After transfection, cells were cultured for 48 to 72 hours before electrophysiological re-

cordings. Single-channel recordings were done in the excised inside-out membrane patch configuration, as described (7) [Y. Tsuura *et al.*, *Diabetes* **42**, 861 (1992)]. The intracellular solution contained 110 mM potassium aspartate, 30 mM KCl, 2 mM $MgSO_4$, 1 mM EGTA, 0.084 mM $CaCl_2$, and 10 mM MOPS (pH 7.2). Dipotassium ATP (1 μM) was always added to the intracellular solution. The pipette solution contained 140 mM KCl, 2 mM $CaCl_2$, and 5 mM MOPS (pH 7.4). Recordings were made at 20° to 22°C.

23. COSm6 cells were plated at a density of 2.5×10^5 cells per well (30-mm six-well dish) and cultured in DMEM (high glucose) (DMEM-HG) supplemented with fetal calf serum (10 percent). The following day, pCMVmBIR (5 μg) and haSUR cDNA (5 μg), cloned into the pECE expression vector (5), were cotransfected into COSm6 cells with DEAE-dextran (5 mg/ml). Cells were incubated for 2 min in Hepes-buffered salt solution containing dimethyl sulfoxide (10 percent) and for 4 hours in DMEM-HG containing fetal bovine serum (FBS) (2 percent) and chloroquine (10 μM) and then returned to DMEM-HG containing FBS (10 percent). After 24 hours, $^{86}RbCl$ (1 μCi/ml) was added in fresh DMEM-HG containing FBS (10 percent). Cells were incubated for 12 to 24 hours before efflux was measured as described (18). Briefly, cells were incubated for 30 min at 25°C in Krebs-Ringer solution containing $^{86}RbCl$ (1 μCi/ml) with or without oligomycin (2.5 μg/ml) and 1 mM 2-deoxy-D-glucose. Cells were washed once in Rb-free Krebs-Ringer solution, with or without added metabolic inhibitors and glibenclamide. Time points were taken by removing all the medium from the cells and replacing it with fresh medium. Portions of the medium from each time point were counted, and the values were summed to determine flux. The data are presented as the percentage of total cellular $^{86}Rb^+$ released. Dose-response curves were obtained with sulfonylureas with metabolic inhibitors or diazoxide without metabolic inhibitors. The percent response was estimated from the efflux values at 40 min; the end points were used as 0 and 100 percent response, respectively. All of the curves are the averages of two or more independent experiments; the error bars are standard deviations. Efficiencies of transfection, estimated from β-galactosidase staining and by recording ATP-sensitive potassium channel activity from excised inside-out patches from randomly chosen cells, were >75 percent and 34 out of 35, respectively. These high levels of transfection gave patches with large numbers of K_{ATP} channels and were unsuitable for recording single channels.
24. N. C. Sturgess, R. Z. Kozlowski, C. A. Carrington, C. N. Hales, M. L. J. Ashford, *Br. J. Pharmacol.* **95**, 83 (1988).
25. G. Trube, P. Rorsman, T. Ohno-Shsaku, *Pfluegers Arch.* **407**, 493 (1986).
26. The plasmid pGEM3Z (Promega) containing a full-length cDNA encoding mBIR and pBluescript SK(+) containing a full-length cDNA encoding haSUR were linearized with Hind III and with Spe I, respectively, and transcribed in vitro, according to the manufacturer's instructions. *Xenopus* oocytes were treated with collagenase, and defolliculated oocytes were selected under microscopy [F. Wibrand *et al.*, *Proc. Natl. Acad. Sci. U.S.A.* **89**, 5133 (1992)]. *Xenopus* oocytes were injected with 60 nl of H_2O alone, mBIR cRNA alone (20 ng), haSUR cRNA alone (40 ng), or mBIR cRNA (20 ng) and haSUR cRNA (40 ng). After 2 to 3 days, electrophysiological measurements were made with the two-electrode voltage clamp technique, as described (7). The microelectrodes were filled with 3 M KCl; the resistance was 0.3 to 1.0 megohm. The extracellular bathing solution contained 90 mM KCl, 3 mM $MgCl_2$, and 5 mM Hepes (pH 7.4). Recordings were made at 20° to 22°C.
27. N. Namba *et al.*, unpublished data.
28. N. Namba *et al.*, unpublished results.
29. D. L. Cook and C. N. Hales, *Nature* **311**, 271 (1984); I. Findlay, M. J. Dunne, O. H. Petersen, *J. Membr. Biol.* **88**, 165 (1985); P. Rorsman and G. Trube, *Pfluegers Arch.* **405**, 305 (1985); S. Misler, L. C. Falke, K. Gillis, M. L. McDaniel, *Proc. Natl. Acad. Sci. U.S.A.* **83**, 7119 (1986).
30. Y. Yamada *et al.*, *Proc. Natl. Acad. Sci. U.S.A.* **89**, 251 (1992).
31. The nucleotide sequences have been deposited in the Genome Sequence Data Base, the DNA Data Bank of Japan, the European Molecular Biology Laboratory, and the National Center for Biotechnology Information nucleotide sequence databases with the accession numbers D50581 and D50582 for the mBIR cDNA and the hBIR gene, respectively.

32. We thank Y. Tsuura and Y. Kubo for contributing to an initial part of the electrophysiological studies, D. Cook for helpful discussion, and K. Sakurai, A. Tamamoto, H. Aida, R. Lee, and M. Lopez for technical assistance. Supported by Scientific Research Grants from the Ministry of Education, Science and Culture and from the Ministry of Health and Welfare, Japan; by grants from Ohtsuka Pharmaceutical Ltd., Novo Nordisk Pharma Ltd., Yamanouchi Foundation for Research on Metabolic Disorders, and NIH (grant DK44311) (J.B.); and by the Houston Endowment (L.A.-B.).

21 August 1995; accepted 19 October 1995

Crystal Structure of the Xanthine Oxidase–Related Aldehyde Oxido-Reductase from *D. gigas*

Maria J. Romão, Margarida Archer, Isabel Moura, José J. G. Moura, Jean LeGall, Richard Engh, Monika Schneider, Peter Hof, Robert Huber*

The crystal structure of the aldehyde oxido-reductase (Mop) from the sulfate reducing anaerobic Gram-negative bacterium *Desulfovibrio gigas* has been determined at 2.25 Å resolution by multiple isomorphous replacement and refined. The protein, a homodimer of 907 amino acid residues subunits, is a member of the xanthine oxidase family. The protein contains a molybdopterin cofactor (Mo-co) and two different [2Fe-2S] centers. It is folded into four domains of which the first two bind the iron sulfur centers and the last two are involved in Mo-co binding. Mo-co is a molybdenum molybdopterin cytosine dinucleotide. Molybdopterin forms a tricyclic system with the pterin bicycle annealed to a pyran ring. The molybdopterin dinucleotide is deeply buried in the protein. The *cis*-dithiolene group of the pyran ring binds the molybdenum, which is coordinated by three more (oxygen) ligands.

Molybdenum is an essential element for microbial, plant, and animal life. Except in the nitrogenases where it is part of a heterometal molybdenum-iron-sulfur cluster, the metal is usually associated with a pterin derivative to form the molybdenum cofactor (Mo-co) (*1*). Mo-co containing enzymes participate in hydroxylation and oxo-transfer reactions that are two-electron transfer processes occurring at the Mo-co site. Water is the ultimate source of the oxygen atom incorporated into the substrate, and reducing equivalents are generated in this process. These features are characteristic of the molybdenum containing hydroxylases and differ from other dioxygen consuming systems. Mo-co enzymes usually contain other redox-active cofactors, such as iron-sulfur clusters, flavins or heme centers, which mediate electron transfer from Mo-co to the final electron acceptor (*1*, *2*).

The aldehyde oxido-reductase (Mop) from the sulfate reducing anaerobic bacterium *Desulfovibrio gigas* contains Mo-co and two different iron-sulfur centers defined by electron paramagnetic resonance (EPR) and Mössbauer spectroscopies as [2Fe-2S] clusters (*3*). This protein was characterized and crystallized (*4*), and its gene was cloned and sequenced (*5*), revealing its relation to xanthine oxidases.

Mop is a homodimer with 907 amino acid residues per monomer. It oxidizes aldehydes to carboxylic acids, with little specificity for the nature of the side group. Mop is part of an electron transfer chain, consisting of four proteins from *D. gigas*, flavodoxin, cytochrome, and hydrogenase such that the oxidation of aldehydes is linked to the generation of hydrogen (*6*). In xanthine oxidases, which have about 1300 amino acid residues, there is electron transfer from the Mo site to a flavin group, associated with a large protein domain absent in Mop.

Chemical studies of derivatives of molybdopterin isolated from xanthine oxidase and

M. J. Romão and M. Archer are at the Instituto de Tecnologia Química e Biológica, Rua da Quinta Grande, 2780 Oeiras and I. S. T., Departamento Química, 1096 Lisboa Codex, Portugal. I. Moura and J. J. G. Moura are in the Departamento de Química (and CQFB) Faculdade de Ciências e Tecnologia, Universidade Nova de Lisboa, 2825 Monte de Caparica, Portugal. J. LeGall is in the Department of Biochemistry and Molecular Biology, University of Georgia, Athens GA 30602, USA. R. Engh, M. Schneider, P. Hof, and R. Huber are at the Max-Planck-Institut für Biochemie, Am Klopferspitz, D-82152 Martinsried, Germany.

*To whom correspondence should be addressed.